Biochimica et Biophysica Acta 1844 (2014) 778–784

Contents lists available at ScienceDirect

Biochimica et Biophysica Acta

journal homepage: www.elsevier.com/locate/bbapap

Arg279 is the key regulator of coenzyme selectivity in the flavin-dependent ornithine monooxygenase SidA☆

Reeder Robinson [a], Stefano Franceschini [b], Michael Fedkenheuer [a], Pedro J. Rodriguez [a], Jacob Ellerbrock [a], Elvira Romero [a,1], Maria Paulina Echandi [a], Julia S. Martin del Campo [a], Pablo Sobrado [a,c,*]

[a] Department of Biochemistry, Virginia Tech, Blacksburg, VA 24061, United States
[b] Department of Biology and Biotechnology, University of Pavia, Via Ferrata 9, 27100, Italy
[c] Virginia Tech Center for Drug Discovery, Virginia Tech, Blacksburg, VA 24061, United States

ARTICLE INFO

Article history:
Received 17 December 2013
Received in revised form 29 January 2014
Accepted 6 February 2014
Available online 15 February 2014

Keywords:
Flavin-dependent monooxygenases
SidA
Aspergillus fumigatus
C4a-hydroperoxyflavin
Coenzyme selectivity
NADPH

ABSTRACT

Siderophore A (SidA) is a flavin-dependent monooxygenase that catalyzes the NAD(P)H- and oxygen-dependent hydroxylation of ornithine in the biosynthesis of siderophores in *Aspergillus fumigatus* and is essential for virulence. SidA can utilize both NADPH or NADH for activity; however, the enzyme is selective for NADPH. Structural analysis shows that R279 interacts with the 2′-phosphate of NADPH. To probe the role of electrostatic interactions in coenzyme selectivity, R279 was mutated to both an alanine and a glutamate. The mutant proteins were active but highly uncoupled, oxidizing NADPH and producing hydrogen peroxide instead of hydroxylated ornithine. For wtSidA, the catalytic efficiency was 6-fold higher with NADPH as compared to NADH. For the R279A mutant the catalytic efficiency was the same with both coenyzmes, while for the R279E mutant the catalytic efficiency was 5-fold higher with NADH. The effects are mainly due to an increase in the K_D values, as no major changes on the k_{cat} or flavin reduction values were observed. Thus, the absence of a positive charge leads to no coenzyme selectivity while introduction of a negative charge leads to preference for NADH. Flavin fluorescence studies suggest altered interaction between the flavin and $NADP^+$ in the mutant enzymes. The effects are caused by different binding modes of the coenzyme upon removal of the positive charge at position 279, as no major conformational changes were observed in the structure for R279A. The results indicate that the positive charge at position 279 is critical for tight binding of NADPH and efficient hydroxylation.

1. Introduction

Fungi from *Aspergillus spp.* are opportunistic human pathogens that cause bronchopulmonary infections in immunocompromised individuals and represent a significant health risk to patients in intensive care units [1]. *Aspergillus fumigatus* is the most common human fungal pathogen and the mortality rate for *Aspergillus*-related infections is >50% [1,2]. It has been shown that during infection, *A. fumigatus* synthesizes and secretes siderophores to scavange iron from the mammalian host. Since iron is required for growth, enzymes in the biosynthesis of siderophores have been identified as potential drug targets [3,4]. Ferricrocin and triacetylfusarinine C are hydroxamate-containing siderophores that are required for virulence [5–7]. In the biosynthesis of these siderophores, N^5-hydroxyornithine is essential for the formation of the hydroxamate iron binding site.

The flavin-dependent monooxygenase siderophore A (SidA), catalyzes the hydroxylation of ornithine to N^5-hydroxyornithine. SidA utilizes NAD(P)H to reduce the flavin cofactor in order to react with molecular oxygen to form a C4a-hydroperoxyflavin intermediate, which is the hydroxylating species (Scheme 1) [8–10]. The formation and stabilization of the C4a-hydroperoxyflavin is critical for hydroxylation. In the absence of ornithine, this intermediate is very stable, eventually decaying to hydrogen peroxide and oxidized flavin (half-life of ~30 min) [8,10,11]. Rapid turnover only occurs when ornithine is present. Stabilization of the C4a-hydroperoxyflavin intermediate ensures that the enzyme couples NADPH oxidation and oxygen activation with ornithine hydroxylation [9,10]. SidA is also able to use NADH, however, the K_M value is 10-fold higher than for NADPH. In addition, the enzyme is only ~50% coupled with NADH while with NADPH the coupling is ~95% [9]. This difference led us to explore the structural determinants of coenzyme selectivity in SidA. Here, we present biochemical and structural data which show that R279 is the key regulator of coenzyme selectivity in SidA.

☆ This work was supported by a grant from the National Science Foundation MCB-1021384.

* Corresponding author at: Department of Biochemistry, Virginia Tech, Blacksburg, VA, 24061, United States. Tel.: +1 540 231 9485; fax: +1 540 231 9070.
E-mail address: psobrado@vt.edu (P. Sobrado).
[1] Present Address: Department of Chemistry, Georgia State University, Atlanta, GA 30302.

http://dx.doi.org/10.1016/j.bbapap.2014.02.005
1570-9639/

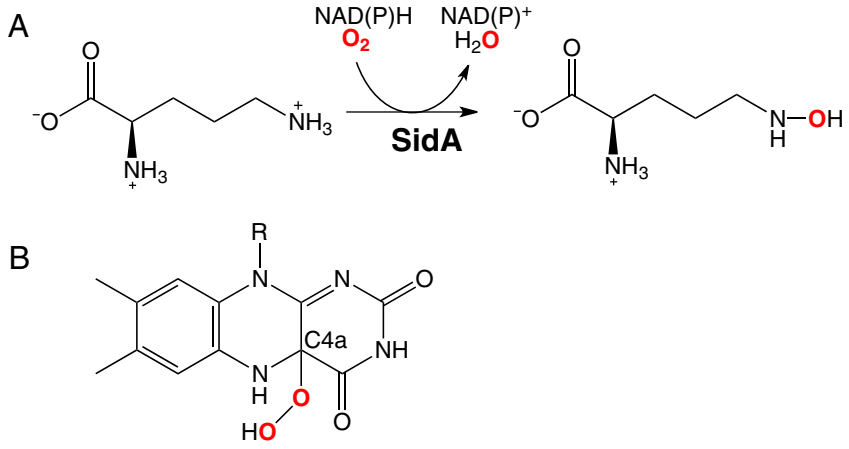

Scheme 1. A) Reaction catalyzed by SidA. B) Structure of the catalytic intermediate C4a-hydroperoxyflavin.

2. Materials and methods

2.1. Materials

Buffers and media were obtained from Fisher Scientific (Pittsburgh, PA). BL21(DE3)-T1^R chemically competent cells were obtained from Sigma-Aldrich (St. Louis, MO). NADH and NADPH were obtained from EMD4 Biosciences (Billerica, MA). DNA primers were synthesized by Integrated DNA Technologies (Coralville, IA). Plasmid preparation and gel purification kits were obtained from Qiagen (Valencia, CA). *Escherichia coli* TOP10 chemically competent cells were obtained from Invitrogen (Carlsbad, CA). Chromatography columns were obtained from GE Healthcare.

2.2. Site-directed mutagenesis

Mutagenesis of R279 to Ala or Glu was performed using the QuikChange (Agilent Technologies) method following the manufacturer's instructions. Wild-type SidA (wtSidA) gene, subcloned into the pET15b plasmid, was used as the template for mutagenesis reactions [12]. For the R279A mutation, the forward primer (5′-GCACCACCCTGATC ATGGCCGACTCGGCTATGCGCCC-3′) and reverse primer (5′-GGGCGCAT AGCCGAGTCGGCCATGATCAGGGTGGTGC-3′) were used. For the R279E mutation, the forward primer (5′-CCCGCACCACCCTGATCATGGAAGACT CGGCTATGCGCCC-3′) and reverse primer (5′-GGGCGCATAGCCGA GTCTTCCATGATCAGGGTGGTGCGGG-3′) were used. The codon at position 279 is underlined.

2.3. Protein expression and purification

All mutant proteins were expressed in *E. coli* BL21(DE3)-T1^R cells and purified as previously described [12]. In general, ~25 mg of protein were obtained per liter of autoinduction media. The purified proteins were stored in 100 mM sodium phosphate, 50 mM NaCl, pH 7.5, at −80 °C at a concentration of ~200 μM (based on flavin content) in 30 μL aliquots.

2.4. Determination of Flavin Incorporation

Flavin incorporation was determined by measuring protein concentration via the Bradford assay (BioRad) and comparing it to the protein concentration based on the flavin spectra. SidA concentration based on flavin content was determined using an extinction coeficent of 13.7 mM^{-1} cm^{-1} at 450 nm [9]. Flavin incorporation was generally close to 70% for wtSidA and mutant proteins.

2.5. Steady-state kinetics

The rate of oxygen consumption was measured using a Hansatech Oxygraph system (Norfolk, England). Reactions consisted of a 1 mL volume of 100 mM sodium phosphate, pH 7.5, at 25 °C. The concentration range of NADPH was 0.005–0.5 mM for wtSidA, 0.05–2 mM for R279A, and 0.1–5 mM for R279E. Similarly, the concentration range for NADH was 0.01–3 mM for wtSidA and R279A, and 0.05–5 mM for R279E. L-ornithine was held constant at 15 mM for all assays where NAD(P)H was varied. When L-ornithine was varied, the coenzyme was kept constant at a concentration at least 5-times the K_M value. Reactions were initiated by addition of 2.0 μM of SidA and monitored for 5 min with constant stirring.

Hydroxylated ornithine was monitored using a variation of the Csaky iodine oxidation assay [13,14]. The standard assay buffer contained 104 μL of 100 mM sodium phosphate (pH 7.5) with varying concentrations of L-ornithine (0 to 20 mM) and saturating concentrations of NAD(P)H (at least 5-times the K_M value). Reactions were initiated by addition of 2.0 μM SidA and incubated for 10 min at 25 °C with constant shaking at 750 rpm.

2.6. Pre-steady-state kinetics

All rapid reaction experiments were carried out at 15 °C using an SX-20 stopped-flow spectrophotometer (Applied Photophysics, Leatherhead, UK) in an anaerobic glove box (Coy, Grass Lake, MI). Anaerobic buffer was obtained through repeated cycles of vacuum (10 min) and flushing with O_2-free argon (1 min) for 1 hr. The same procedure was used to make the enzyme anaerobic. Substrates were made anaerobic by dissolving in anaerobic buffer inside the glove box. The rate of flavin reduction was measured by mixing anaerobic SidA (15 μM after mixing) with an equal volume of NADPH at final concentrations of 0.5 mM for wtSidA, 0.05–2 mM for R279A, and 0.5–5 mM for R279E. Reduction by NADH was performed at 0.05–1.5 mM for wtSidA, and 0.05–5 mM for both mutant enzymes. Spectra were taken on a logarithmic time scale until full reduction of the flavin was observed as determined by a decrease in absorbance at 452 nm. The rate constants at various coenzyme concentrations were determined by fitting the changes in absorbance at 452 nm to Eq. (1). In this double exponential equation, a is the change in absorbance, k is the rate, and c is the final absorbance. The resulting values were plotted as a function of reduced coenzyme concentration and the data fit to Eq. (2) to obtain the maximum rate constant of flavin reduction (k_{red}) and the K_D value [15].

$$v = c + a_1 e^{-(k_1 * t)} + a_2 e^{-(k_2 * t)} \quad (1)$$

$$k_{obs} = \frac{k_{red}[NAD(P)H]}{K_D + [NAD(P)H]} \quad (2)$$

2.7. Flavin fluorescence

The effect of oxidized coenzyme binding on flavin fluorescence was determined on a SpectraMax M5e plate reader (Molecular Devices, Sunnyvale, CA). Excitation was performed at 450 nm, and the changes in flavin fluorescence were monitored from 500 to 625 nm. A 495 nm cutoff filter was used for each fluorescence experiment. The standard assay buffer contained 100 μL of 100 mM sodium phosphate, pH 7.5, with 15 μM SidA. For wtSidA, 0.9 mM $NADP^+$ or 4 mM NAD^+ were used. For R279A, 3 mM $NADP^+$ or 5 mM NAD^+ were used. For R279E, 15 mM $NADP^+$ or 5 mM NAD^+ were used.

2.8. Crystallization and structure determination

Crystals of *A. fumigatus* R279A SidA containing L-ornithine were obtained at 4 °C by the vapor diffusion method under the same conditions used for the wild-type protein (reservoir containing 1.6 M ammonium sulfate, 0.1 M HEPES, pH 6.6, 2% dioxane, and a protein solution of 8 mg/ml SidA in 25 mM HEPES, pH 7.5, 100 mM NaCl, 15 mM L-ornithine, 1 mM $NADP^+$ [12]. Data were collected at the European Synchrotron Radiation Facility (Grenoble, France). The structure was solved by molecular replacement starting from the structure of the wild-type enzyme (PDB entry 4B63). All crystallographic calculations were performed with programs of the CCP4 package [16]. Figures were generated using Pymol (www.pymol.org).

3. Results and discussion

Class B flavin-dependent monooxygenases are highly selective for NADPH [17]. Some members of this family, such as phenylacetone monooxygenase (PAMO) and the ornithine hydroxylase from *Pseudomonas aeruginosa* (PvdA), are 100% selective for NADPH as these enzymes are reported to be unable to react with NADH [18,19]. Similarly, the Baeyer–Villiger monooxygenases (BVMOs) cyclohexanone monooxygenase (CHMO) and 4-hydroxyacetophenone monooxygenase (HAPMO) have been shown to be highly selective for NADPH with a 700-fold preference over NADH (based on reported k_{cat}/K_M values) [20]. On the other hand, mammalian flavin-dependent monooxygenase (FMO) and SidA are less selective, with less than 20-fold preference for NADPH [9,21,22]. The x-ray crystal structure of SidA in complex with $NADP^+$ shows that the R279 ion pairs with the 2′-phosphate of $NADP^+$ and the guanidinium group is involved in stacking interactions with the adenine base (Fig. 1) [12]. We probed the role of this residue in coenzyme selectivity using site-directed mutagenesis and subsequent characterization of the resulting mutant enzymes.

The effect of removing the positive charge of R279 on coenzyme selectivity was probed by mutating this residue to alanine. The R279A enzyme was purified following the same procedures as wtSidA. The yield of the purified mutant enzyme was ~25 mg per liter of *E. coli* culture with a flavin content of ~70%. This data is consistent with previously reported values for wtSidA [8,9]. Mutation of R279 to E was also performed in order to introduce a negative charge at this position, which would have a repulsion effect with the 2′-phosphate of NADPH, but not with NADH. The resulting R279E enzyme was purified as the R279A with similar yields. The flavin spectra for both mutants are identical to the flavin spectrum of the wtSidA (not shown).

The kinetic values determined by measuring the rate of oxygen consumption were calculated as a function of coenzyme concentration with ornithine saturating at 15 mM (Fig. 2). The data is summarized in Table 1. The catalytic efficiency with NADPH decreased ~40- and ~300-fold for the R279A and R279E enzymes, respectively. This decrease is mainly due to an increase in the K_M values, since the k_{cat} value was unchanged for the R279A enzyme, while it decreased only by 30% for the R279E enzyme. With NADH, the catalytic efficiencies for R279A and R279E decreased only 7- and 11-fold, respectively. These relatively minor effects are also mainly due to changes in the K_M values. Interestingly, a slight increase in the k_{cat} value for NADH was observed for the R279E enzyme (~30%) (Table 1).

Reduction of the flavin cofactor by NAD(P)H was monitored using a stopped-flow spectrophotometer under anaerobic conditions. We have previously determined that the hydride transfer step occurs in two phases and using stereospecifically labeled (4*R*)-4-^{2}H-NADPH the reaction was shown to be specific for the *pro*-R-hydrogen and a kinetic isotope effect value of ~5.5 was measured in both phases. This indicates that both phases of flavin reduction of wtSidA with NADPH correspond to hydride transfer. The affinity of wtSidA for NADPH is very high, which prevents accurate determination of the K_D value for this coenzyme in the stopped-flow spectrophotometer. Therefore, the K_D value for

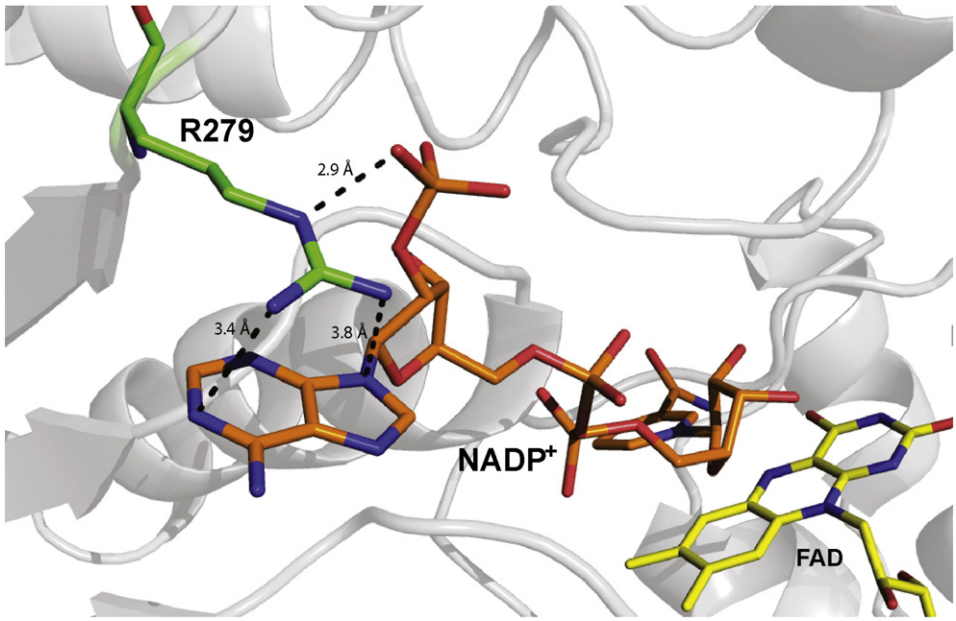

Fig. 1. Interaction of R279 with $NADP^+$. The figure was made using Pymol with PDB entry 4B63.

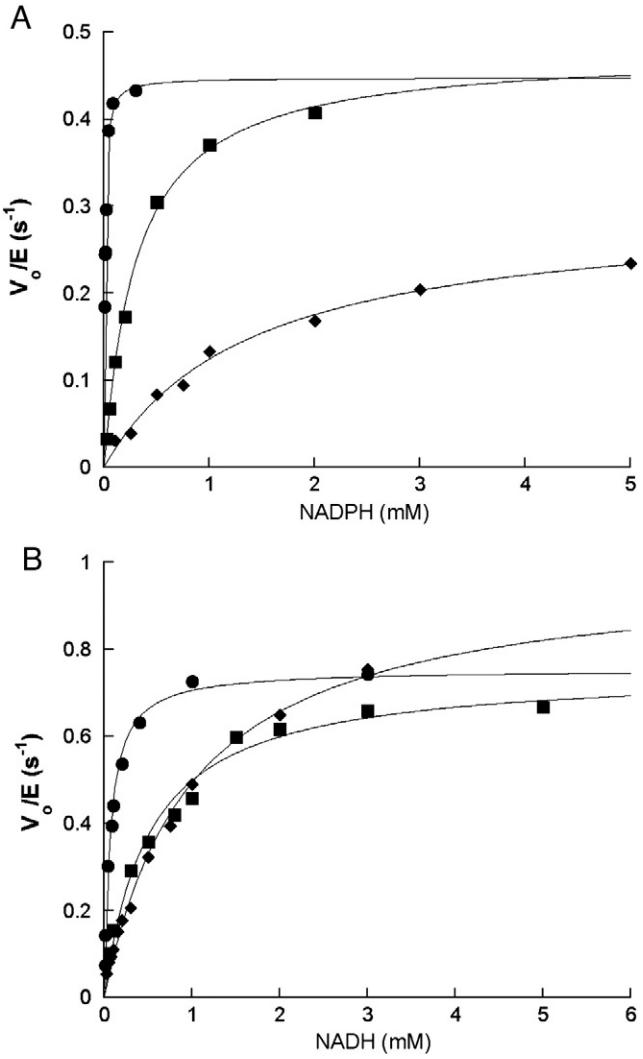

Fig. 2. Initial rate of oxygen consumption as a function of NADPH (A) or NADH (B) for wtSidA (●), R279A (■), and R279E (♦). The assays were performed in 1 mL sodium phosphate, pH 7.5, at 25 °C. The lines are fit to the Michaelis–Menten equation.

NADPH has been estimated to be ~1 μM [10]. The reaction of wtSidA with NADH also occurs in two phases. The first phase is fast, isotope sensitive, and increases as a function of NADH concentration, indicating that it corresponds to flavin reduction. The second phase has a much slower rate and is isotope and concentration independent. Therefore, this phase is believed to correspond to NAD^+ release [8]. With the R279 mutants, the reaction with NADPH also occurs in two phases. The first phase was fast and increased as a function of NADPH concentration, allowing determination of both the k_{red} and K_D values (Fig. 3 and Table 2). This relatively fast phase corresponds to flavin reduction. The second phase was slower (~0.07 s^{-1} for both mutant enzymes)

Table 1
Steady-state kinetic parameters determined by oxygen consumption.

Parameters/variable substrate	Wild-type	R279A	R279E
NADPH			
k_{cat} (s^{-1})	0.45 ± 0.01	0.48 ± 0.01	0.30 ± 0.01
K_M (mM)	0.0070 ± 0.0001	0.31 ± 0.02	1.54 ± 0.20
k_{cat}/K_M (M^{-1} s^{-1})	64,000 ± 5000	1500 ± 100	200 ± 10
NADH			
k_{cat} (s^{-1})	0.75 ± 0.02	0.75 ± 0.03	1.00 ± 0.05
K_M (mM)	0.070 ± 0.007	0.51 ± 0.07	1.0 ± 0.1
k_{cat}/K_M (M^{-1} s^{-1})	11,000 ± 150	1500 ± 100	1000 ± 60

Conditions: 100 mM sodium phosphate, pH 7.5, and 25 °C.

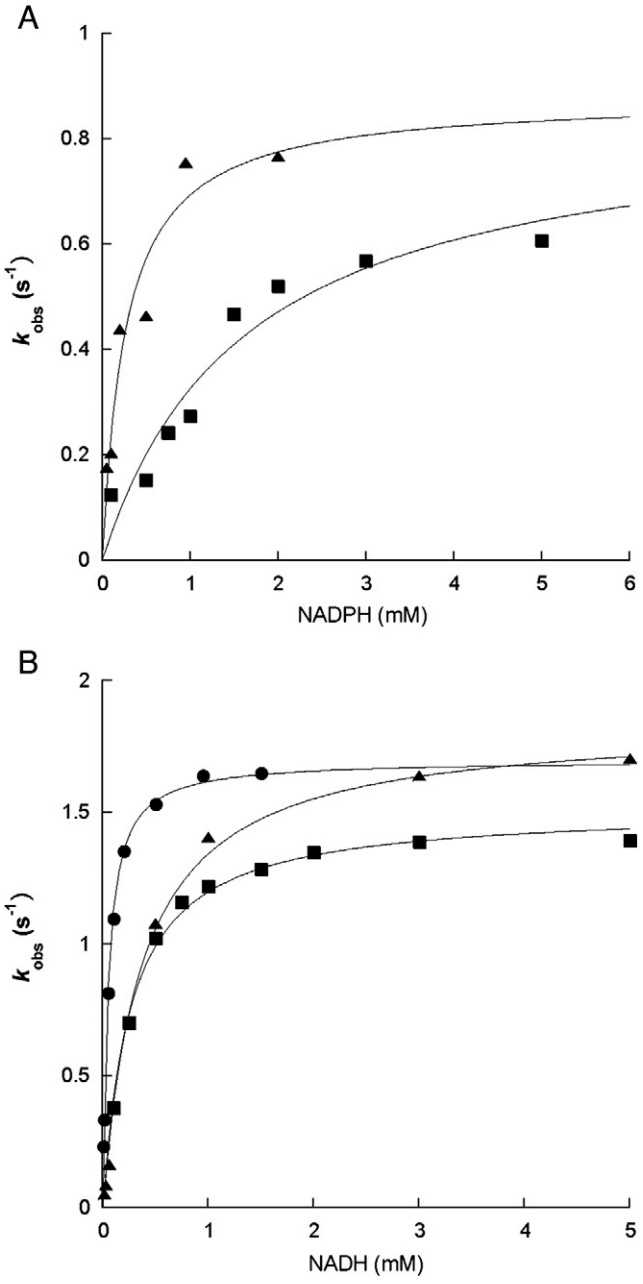

Fig. 3. A) Flavin reduction as a function of NADPH for R279A (▲), and R279E (■). B) Flavin reduction as a function of NADH for wtSidA (●), R279A (▲), and R279E (■). The maximum rate constants for flavin reduction (k_{red}) and the K_D value were obtained by fitting the data to Eq. (2).

and independent of NADPH concentration. We attribute this phase to $NADP^+$ release. The results indicate that alteration of the electrostatic environment at position 279 does not significantly affect the rate of flavin reduction. However, the affinity for NADPH is significantly affected (Table 2). Using the estimate of 1 μM for the K_D value of NADPH for

Table 2
Rate constants for flavin reduction and dissociation constants with NAD(P)H.

	NADPH		NADH	
Enzyme	k_{red} (s^{-1})	K_D (mM)	k_{red} (s^{-1})	K_D (mM)
wtSidA	0.63 ± 0.01	~0.001	1.69 ± 0.01	0.070 ± 0.005
R279A	0.88 ± 0.01	0.27 ± 0.05	1.84 ± 0.04	0.37 ± 0.03
R279E	0.9 ± 0.1	1.6 ± 0.5	1.52 ± 0.02	0.26 ± 0.02

Conditions: 100 mM sodium phosphate, pH 7.5, and 25 °C.

wtSidA, it can be predicted that mutations of R279 changed the K_D for NADPH at least 270-fold for R279A and 1600-fold for R279E (Table 2).

The lower affinity of wtSidA for NADH permits the accurate determination of both the k_{red} and K_D values (Fig. 3). Mutation of R279 resulted in a decrease in K_D values for NADH of only 3.7- to 5-fold. While no significant changes of the k_{red} values with either reduced dinucleotide were observed in the mutant enzymes. Clearly, the modification of R279 is less important for NADH binding. In summary, the steady-state and stopped-flow kinetic analyses of the R279A/E enzymes show that removal of the positive charge at position 279 significantly decreases the affinity for NADPH. Comparison of the catalytic efficiencies of the R279A enzyme with NADPH and NADH clearly shows no substrate selectivity. Furthermore, in the R279E enzyme, the coenzyme selectivity is reversed, favoring NADH by 5-fold.

The activity of wtSidA and the R279 mutants were also determined by following ornithine hydroxylation (Table 3). As expected, the K_M value for ornithine did not significantly change in the R279 mutants. However, the k_{cat} values for the R279A and R279E mutants decreased by ~2–6 fold (Table 3). The decrease in the k_{cat} values could originate from uncoupling. If only some of the oxygen that is consumed in the reaction leads to hydroxylation of ornithine, and the rest is released as hydrogen peroxide, a lower rate of ornithine hydroxylation would be measured. Coupling of the enzymatic reaction was determined by dividing the turnover value from the oxygen consumption assay with the turnover value calculated in the hydroxylation assay. For wtSidA, coupling with NADPH is greater than 90%, but with NADH, coupling decreases to 50%. With the R279 mutants, the coupling is only between ~25 and 60% (Table 3). These results indicate that the positive charge is essential for efficient hydroxylation and for minimizing production of hydrogen peroxide. In SidA and other flavin-containing monooxygenases, NADPH remains bound throughout the catalytic cycle [9,10,23–25]. This is strictly required because NADP(H) plays a role in reducing the flavin, and stabilizing the C4a-hydroperoxyflavin. For wtSidA, the decrease in coupling with NADH can be attributed to a faster k_{off}, which in turn leads to fast decay of the C4a-hydroperoxyflavin. Similarly, in the mutant enzymes, since coenzyme binding affinity is lower, the decrease in coupling can be attributed at least in part to $NAD(P)^+$ being released prior to hydroxylation of ornithine.

The structure of R279A was solved by x-ray crystallography at 2.0 Å resolution (Table 4). The enzyme was crystallized under the same conditions as wtSidA in the presence of ornithine and $NADP^+$. The structure of R279A is virtually identical to that of wtSidA with a root-mean-square deviation for the Cα atoms of 0.22 Å (with reference to PDB entry 4B63). The conformation of the alanine mutation is the same as for the Arg279 side chain of wtSidA (Fig. 4). The major difference between the crystal structures of wtSidA and R279A is the absence of electron density for $NADP^+$, which might be due to the lower binding affinity. We noticed minor differences on the side chain of some residues in the loop region that is close to the binding site of $NADP^+$, most notably Tyr324 (not shown). Clearly, no major conformational changes are observed in the structure of R279A. Thus, the decrease in binding is directly due to the lack of ionic interaction in the mutant protein.

Table 3
Steady-state kinetic parameters following ornithine hydroxylation.

Parameter/variable substrate	wtSidA	R279A	R279E
Ornithine[a]			
k_{cat} (s^{-1})	0.41 ± 0.01	0.25 ± 0.01	0.170 ± 0.003
K_M (mM)	0.65 ± 0.10	1.0 ± 0.2	0.72 ± 0.16
k_{cat}/K_M (M^{-1} s^{-1})	700 ± 100	260 ± 40	220 ± 40
% coupling	91	52	56
Ornithine[b]			
k_{cat} (s^{-1})	0.40 ± 0.01	0.19 ± 0.01	0.070 ± 0.003
K_M (mM)	0.72 ± 0.11	1.0 ± 0.2	0.08 ± 0.01
k_{cat}/K_M (M^{-1} s^{-1})	560 ± 70	200 ± 30	220 ± 20
% coupling	53	25	34

Conditions: 100 mM sodium phosphate, pH 7.5, and 25 °C. Assays were performed at five times the K_M value for [a]NADPH or [b]NADH.

Table 4
Crystallographic statistics.

	R279A
PDB code	4NZH
unit cell axes (Å)[a]	77.9, 84.1, 144.9
resolution (Å)	2.0
R_{merge} (%)[b,c]	9.3 (61.9)
completeness (%)[c]	99.0 (97.1)
unique reflections	30,804
redundancy	15.5 (15.0)
$I/\sigma(I)$[c]	29.6 (3.7)
R_{cryst} (%)	20.7
R_{free} (%)	24.3
rmsd bond lengths (Å)	0.005
rmsd bond angles (°)	1

[a] Space group is I222.
[b] $R_{merge} = \Sigma|I_i - \langle I \rangle|/\Sigma I_i$, where I_i is the intensity of i^{th} observation and <I> is the mean intensity of the reflection.
[c] Values in parentheses are for reflections in the highest resolution shell.

Intrinsic flavin fluorescence was used as a probe of the interaction between the nicotinamide ring and the isoalloxazine ring of FAD. With wtSidA, binding of $NADP^+$ causes a decrease in flavin fluorescence. In contrast, binding of NAD^+ causes an increase in flavin fluorescence (Fig. 5) [8]. Clearly, the interaction between the oxidized co-enzymes and the flavin is not the same, which results in differences in the flavin environment that can be detected by flavin fluorescence. As observed in the wtSidA structure in complex with $NADP^+$, the nicotinamide ring binds adjacent to the isoalloxazine ring. Thus, this interaction might be responsible for the observed quenching of the flavin fluorescence. It is possible that with NAD^+, the nicotinamide ring is not binding so close to the flavin as to cause fluorescence quenching, but instead makes the active site more hydrophobic, which would enhance flavin fluorescence (Fig. 5). With the R279 mutants, NAD^+ binding causes a similar increase in the fluorescence, consistent with the results for wtSidA. In contrast, the binding of $NADP^+$ no longer quenches the fluorescence, but increases fluorescence in the mutant enzymes. These results suggest that interaction between R279 and the 2′-phosphate has an effect in the interaction of the nicotinamide ring and the flavin in the active site.

A structurally homologous arginine is conserved in other Class B flavin-dependent monooxygenases such as FMO, CHMO, and PvdA [23,26,27]. As mentioned previously, PvdA has been reported to not recognize NADH as a substrate. This is surprising since the structure of PvdA and SidA are almost identical with an RMS of 1.049 Å. It is possible that protein dynamics important for NADPH binding are different between these two enzymes, however, this remains to be tested. In FMO, the role of the conserved Arg residue has not been determined. Based on amino acid sequence alignment, several positively charged residues were targeted for mutagenesis in order to determine coenzyme selectivity in HAPMO from *Pseudomonas fluorescens* ACB [20]. Replacement of R339 with alanine (equivalent to R279 in SidA) resulted in a shift of the selectivity from NADPH to NADH. However, the selectivity originated from an almost complete loss of activity with NADPH. Thus, the interactions between an Arg residue and the 2′-phosphate of NADPH play different roles in HAPMO as compared to SidA. In addition, it was also shown that a lysine residue (K439) in HAPMO is also important for coenzyme selectivity. Mutagenesis of K439 to alanine decreased the selectivity for NADPH by ~100-fold. In CHMO from *Acinetobacter* sp. NCBI 9871, another BVMO, a lysine residue (K326) has also been shown to be involved in coenzyme selectivity. Characterization of the CHMO K326A mutant showed a decrease in the selectivity for NADPH of more than 50-fold [20]. The three-dimensional structure of CHMO was later solved and showed that K326 is in hydrogen bonding distance to the 2′-phosphate of $NADP^+$ [27]. The structure of SidA does not show the presence of another positively charged residue in close proximity

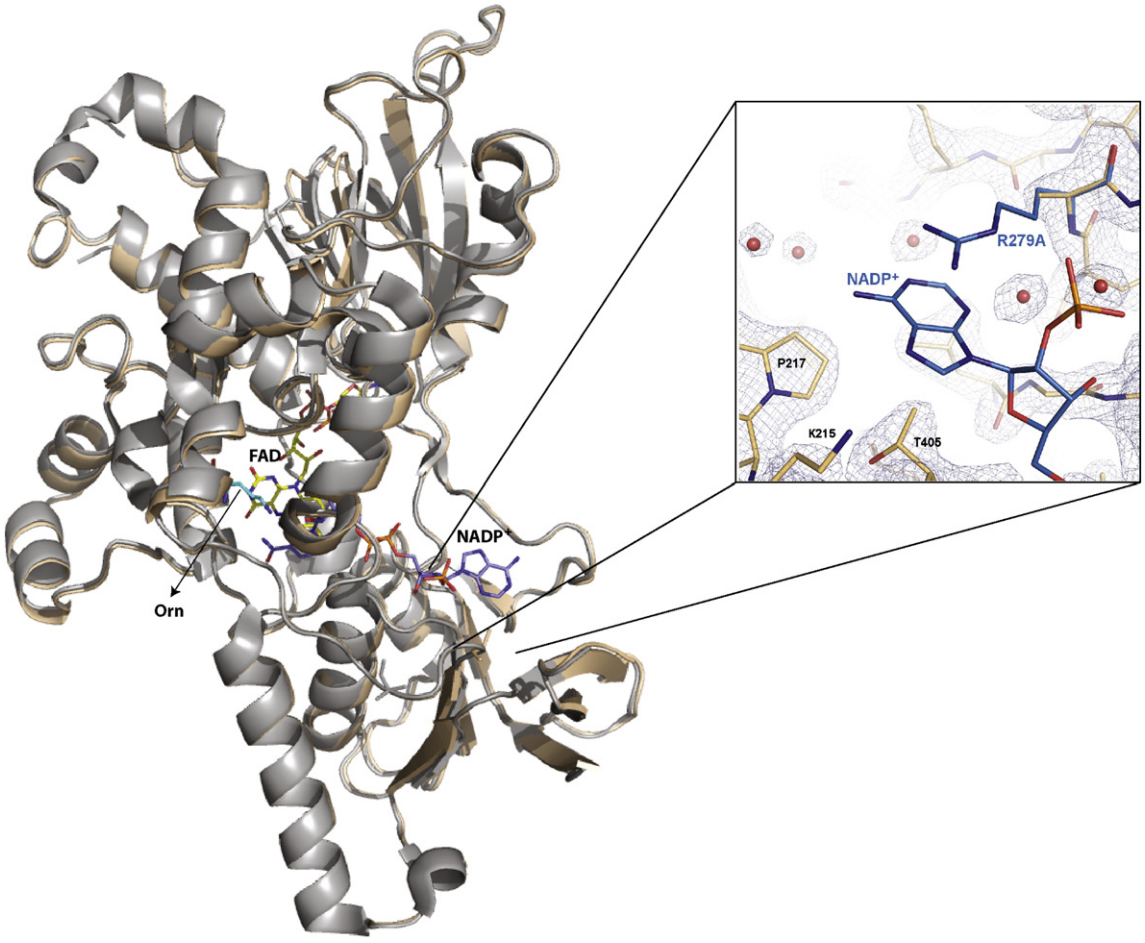

Fig. 4. Superposition of the structure of wtSidA (gray) and R279A (gold). The FAD and Orn in R279A are those found in the structure of R279A. The $NADP^+$ is only observed in wtSidA (PDB entry 4B63). The insert shows the 2Fo–Fc weighted electron density map around the site of the R279A mutation contoured at the 1.4 σ level. The picture also shows the conformation of R279 and bound $NADP^+$ as observed in the wild-type enzyme (light blue carbons; PDB entry 4B63).

to the 2′-phosphate of $NADP^+$. The large decrease in activity upon mutation of the R339 in HAPMO and the role of another positive residue indicates that the mechanism of coenzyme selectivity in BVMOs is more complex than in SidA.

In summary, the biochemical characterization of the R279 mutants clearly shows that this residue plays a key role in coenzyme selectivity. Removal of the positive charge at this position abolishes the ability to preferentially bind NADPH and the addition of a negative charge shifts the coenzyme selectivity to NADH. Even though this residue is not near the active site, the reaction becomes significantly uncoupled in the mutant enzymes. This can be attributed, in part, to the release of $NAD(P)^+$ from the active site due to the decrease in affinity. The changes in flavin fluorescence indicate that the interaction between $NADP^+$ and the flavin is modified upon mutation. Therefore, it is possible that

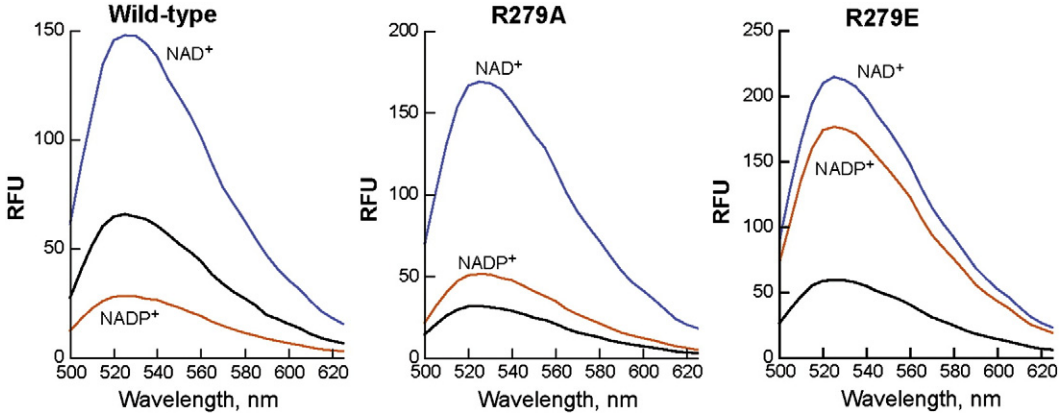

Fig. 5. Changes in flavin fluorescence induced by oxidized coenzyme binding. The oxidized flavin fluorescence was excited at 450 nm. The emission of the free enzymes (black lines) or when bound to $NADP^+$ (orange) or NAD^+ (blue) were recorded from 500 to 630 nm.

mutation of R279, in addition to affecting the binding affinity, also affects the positioning of $NADP^+$, which is required for optimal stabilization of the C4a-hydroperoxyflavin in SidA.

Acknowledgments

This work was supported by a grant from the National Science Foundation MCB-1021384.

References

[1] H. He, L. Ding, F. Li, Q. Zhan, Clinical features of invasive bronchial–pulmonary aspergillosis in critically ill patients with chronic obstructive respiratory diseases: a prospective study, Crit. Care 15 (2011) R5.
[2] A. Abad, J.V. Fernandez-Molina, J. Bikandi, A. Ramirez, J. Margareto, J. Sendino, F.L. Hernando, J. Ponton, J. Garaizar, A. Rementeria, What makes *Aspergillus fumigatus* a successful pathogen? Genes and molecules involved in invasive aspergillosis, Rev. Iberoam. Micol. 27 (2010) 155–182.
[3] H. Haas, Iron — a key nexus in the virulence of *Aspergillus fumigatus*, Front. Microbiol. 3 (2012) 28.
[4] H. Haas, M.m Eisendel, B.G. Turgeon, Siderophores in fungal physiology and virulence, Annu. Rev. Phytopathol. 46 (2008) 149–187.
[5] A. Wallner, M. Blatzer, M. Schrettl, B. Sarg, H. Lindner, H. Haas, Ferricrocin, a siderophore involved in intra- and transcellular iron distribution in *Aspergillus fumigatus*, Appl. Environ. Microbiol. 75 (2009) 4194–4196.
[6] M. Eisendle, H. Oberegger, I. Zadra, H. Haas, The siderophore system is essential for viability of Aspergillus nidulans: functional analysis of two genes encoding l-ornithine N 5-monooxygenase (sidA) and a non-ribosomal peptide synthetase (sidC), Mol. Microbiol. 49 (2003) 359–375.
[7] A.H. Hissen, A.N. Wan, M.L. Warwas, L.J. Pinto, M.M. Moore, The *Aspergillus fumigatus* siderophore biosynthetic gene sidA, encoding L-ornithine N5-oxygenase, is required for virulence, Infect. Immun. 73 (2005) 5493–5503.
[8] E. Romero, M. Fedkenheuer, S.W. Chocklett, J. Qi, M. Oppenheimer, P. Sobrado, Dual role of NADP(H) in the reaction of a flavin dependent N-hydroxylating monooxygenase, Biochim. Biophys. Acta 1824 (2012) 850–857.
[9] S.W. Chocklett, P. Sobrado, Aspergillus fumigatus SidA is a highly specific ornithine hydroxylase with bound flavin cofactor, Biochemistry 49 (2010) 6777–6783.
[10] J.A. Mayfield, R.E. Frederick, B.R. Streit, T.A. Wencewicz, D.P. Ballou, J.L. DuBois, Comprehensive spectroscopic, steady state, and transient kinetic studies of a representative siderophore-associated flavin monooxygenase, J. Biol. Chem. 285 (2010) 30375–30388.
[11] E. Romero, D. Avila, P. Sobrado, Effect of pH on the Reductive and Oxidative Half-reactions of Aspergillus fumigatus Siderophore A, in: S. Miller, R. Hille, B. Palfey (Eds.), In Flavins and Flavoproteins, Lulu, Raleigh, NC, 2013, pp. 289–294.
[12] S. Franceschini, M. Fedkenheuer, N.J. Vogelaar, H.H. Robinson, P. Sobrado, A. Mattevi, Structural insight into the mechanism of oxygen activation and substrate selectivity of flavin-dependent N-hydroxylating monooxygenases, Biochemistry 51 (2012) 7043–7045.
[13] T. Csaky, On the estimation of bound hydroxylamine in biological materials, Acta Chem. Scand. 2 (1948) 450–454.
[14] R. Robinson, P. Sobrado, Substrate binding modulates the activity of *Mycobacterium smegmatis* G (MbsG), a flavin-dependent monooxygenase involved in the biosynthesis of hydroxamate-containing siderophores, Biochemistry 50 (2011) 8449–8496.
[15] S. Strickland, G. Palmer, V. Massey, Determination of dissociation constants and specific rate constants of enzyme-substrate (or protein–ligand) interactions from rapid reaction kinetic data, J. Biol. Chem. 250 (1975) 4048–4052.
[16] M.D. Winn, C.C. Ballard, K.D. Cowtan, E.J. Dodson, P. Emsley, P.R. Evans, R.M. Keegan, E.B. Krissinel, A.G. Leslie, A. McCoy, S.J. McNicholas, G.N. Murshudov, N.S. Pannu, E.A. Potterton, H.R. Powell, R.J. Read, A. Vagin, K.S. Wilson, Overview of the CCP4 suite and current developments, Acta Crystallogr. D Biol. Crystallogr. 67 (2011) 235–242.
[17] W.J. van Berkel, N.M. Kamerbeek, M.W. Fraaije, Flavoprotein monooxygenases, a diverse class of oxidative biocatalysts, J. Biotechnol. 124 (2006) 670–689.
[18] K.M. Meneely, A.L. Lamb, Biochemical characterization of a flavin adenine dinucleotide-dependent monooxygenase, ornithine hydroxylase from *Pseudomonas aeruginosa*, suggests a novel reaction mechanism, Biochemistry 46 (2007) 11930–11937.
[19] M.W. Fraaije, J. Wu, D.P. Heuts, E.W. van Hellemond, J.H. Spelberg, D.B. Janssen, Discovery of a thermostable Baeyer–Villiger monooxygenase by genome mining, Appl. Microbiol. Biotechnol. 66 (2005) 393–400.
[20] N.M. Kamerbeek, M.W. Fraaije, D.B. Janssen, Identifying determinants of NADPH specificity in Baeyer–Villiger monooxygenases, Eur. J. Biochem. 271 (2004) 2107–2116.
[21] N.B. Beaty, D.P. Ballou, The reductive half-reaction of liver microsomal FAD-containing monooxygenase, J. Biol. Chem. 256 (1981) 4611–4618.
[22] N.B. Beaty, D.P. Ballou, Transient kinetic study of liver microsomal FAD-containing monooxygenase, J. Biol. Chem. 255 (1980) 3817–3819.
[23] A. Alfieri, E. Malito, R. Orru, M.W. Fraaije, A. Mattevi, Revealing the moonlighting role of NADP in the structure of a flavin-containing monooxygenase, Proc. Natl. Acad. Sci. U. S. A. 105 (2008) 6572–6577.
[24] D.E. Torres Pazmino, B.J. Baas, D.B. Janssen, M.W. Fraaije, Kinetic mechanism of phenylacetone monooxygenase from *Thermobifida fusca*, Biochemistry 47 (2008) 4082–4093.
[25] L.L. Poulsen, D.M. Ziegler, The liver microsomal FAD-containing monooxygenase. Spectral characterization and kinetic studies, J. Biol. Chem. 254 (1979) 6449–6455.
[26] J. Olucha, K.M. Meneely, A.S. Chilton, A.L. Lamb, Two structures of an N-hydroxylating flavoprotein monooxgenase: the ornithine hydroxylase from *Pseudomonas aeruginosa*, J. Biol. Chem. 286 (2011) 31789–31798.
[27] I.A. Mirza, B.J. Yachnin, S. Wang, S. Grosse, H. Bergeron, A. Imura, H. Iwaki, Y. Hasegawa, P.C. Lau, A.M. Berghuis, Crystal structures of cyclohexanone monooxygenase reveal complex domain movements and a sliding cofactor, J. Am. Chem. Soc. 131 (2009) 8848–8854.